Is the uniform electron gas limit important for small Ag clusters? Assessment of different density functionals for Agn (n 4)

Shuang Zhao, Zhen-Hua Li, Wen-Ning Wang, Zhi-Pan Liu, Kang-Nian Fan et al.

Additional information on J. Chem. Phys.

Is the uniform electron gas limit important for small Ag clusters? Assessment of different density functionals for Ag_n ($n \leq 4$)

Shuang Zhao, Zhen-Hua Li, Wen-Ning Wang, Zhi-Pan Liu, and Kang-Nian Fan[a)]
Shanghai Key Laboratory of Molecular Catalysis and Innovative Materials, Department of Chemistry, Center for Theoretical Chemical Physics, Fudan University, Shanghai 200433, People's Republic of China

Yaoming Xie and Henry F. Schaefer III[b)]
Center for Computational Chemistry, University of Georgia, Athens, Georgia 30606

Twenty-three density functional theory (DFT) methods, including the second- and the third-generation functionals, are tested in conjunction with two basis sets (LANL2DZ and SDD) for studying the properties of neutral and ionic silver clusters. We find that DFT methods incorporating the uniform electron gas limit in the correlation functional, namely, those with Perdew's correlation functionals (PW91, PBE, P86, and TPSS), Becke's B95, and the Van Voorhis-Scuseria functional VSXC, generally perform better than the other group of functionals, e.g., those incorporating the LYP correlation functional and variations of the B97 functional. Strikingly, these two groups of functionals can produce qualitatively different results for the Ag_3 and Ag_4 clusters. The energetic properties and vibrational frequencies of Ag_n are also evaluated by the different functionals. The present study shows that the choice of DFT methods for heavy metals may be critical. It is found that the exact-exchange-incorporated PBE functional (PBE1PBE) is among the best for predicting the range of properties. © *2006 American Institute of Physics*. [DOI: 10.1063/1.2193512]

I. INTRODUCTION

The reliability of the Kohn-Sham density functional theory (DFT) methods is governed by the quality of the approximate exchange-correlation (XC) energy functional $E_{xc}[\rho]$. In the last decade, a number of new functionals have been deduced, either by fitting the required DFT parameters to match a collection of experimental results or by forcing the functional to satisfy certain exact constraints based on first principles. Recently, many second- and third-generation pure and hybrid DFT methods have been tested on the heats of reaction and reaction barrier heights for organic systems, and some of them have proven to be better than the first-generation methods.[1,2] Interestingly, the assessment of DFT methods on the systems containing transition and coinage metal atoms seems to manifest a more complex picture than that for organic systems.[3–6] For example, the study of Baker and Pulay[5] indicates that there is no real incentive to use O3LYP (Refs. 7 and 8) instead of the popular B3LYP method[8,9] for computations involving molecules containing first-row transition metal atoms, although the former involves a new "optimized" exchange[7] OPTX constructed to produce a more accurate Hartree-Fock (HF) exchange energy for atoms than the B88 (Ref. 10) functional. More recently, 42 different functionals were tested by Schultz *et al.* on eight selected transition metal dimers (Ag_2, Cr_2, Cu_2, CuAg, Mo_2, Ni_2, V_2, and Zr_2).[6] The BLYP method[8,10] was found to be the

most accurate functional for bond energies and reasonably accurate for bond lengths.[6] However, many of these studies involve no more than two atoms of the $3d$ and $4d$ transition metals. To date, comparative studies of new functionals for larger transition metal clusters are still lacking due to the high computational demands. For such systems, reliable predictions of the structures and energies are of paramount importance.

In the present work, we aim to achieve a better understanding on the power and limitations of these new functionals for heavier metal systems, in particular, the relationship between the predicted structural conformations and the exchange and correlation functionals. The silver clusters are chosen as the model systems, as the physical and chemical properties of silver clusters and nanoparticles have attracted much attention for their relevance in catalysis, electrochemistry, heat dissipation, and biofiltration,[11] and there have been previous *ab initio* and DFT studies on these systems.[12–18] A large selection of density functionals, both generalized gradient approximation (GGA) and hybrid, are adopted in our work on the neutral and ionic Ag_n ($n \leq 4$) clusters. The purpose of this research is to begin to formulate general rules for the application of different DFT methods to the realm of transition metal clusters. The reliability of these functionals is evaluated by comparing predicted DFT equilibrium geometries, vibrational frequencies, vertical and adiabatic ionization potentials (VIP and AIP), and vertical detachment energies (VDEs) with available experimental data or high-level *ab initio* results.

[a)]Electronic mail: knfan@fundan.edu.cn
[b)]Electronic mail: hfs@uga.edu

TABLE I. Bond lengths (in Å) and bond angles (in degrees) of Ag$_3$, Ag$_3^-$, and Ag$_3^+$ predicted by different DFT methods with the LANL2DZ basis set. Note that some functionals predict two minima for the $^2B_2$ ground state of Ag$_3$.

| | Ag$_3$(C_{2v}) | | | | Ag$_3^-(D_{3h})$ | Ag$_3^+(D_{\infty h})$ |
| | $^2B_2$ | | | | | |
	R	Angle	R	Angle	R	R
VSXC	2.659	70.8	2.651	164.5	2.675	2.707
PBEPBE	2.664	71.6	2.663	133.9	2.688	2.722
PBE1PBE	2.670	72.1			2.698	2.732
TPSSTPSS	2.649	69.7	2.646	127.9	2.669	2.705
PW91PW91	2.658	71.4	2.656	134.0	2.679	2.716
MPWPW91	2.661	72.1	2.661	135.0	2.684	2.721
MPW1PW91	2.669	72.6			2.695	2.731
MPWB95	2.658	70.0	2.656	138.7	2.679	2.711
OB95	2.682	73.5	2.701	147.5	2.719	2.740
B1B95	2.666	70.5	2.666	125.2	2.693	2.722
BP86	2.655	71.1	2.653	136.3	2.678	2.712
G96VP86	2.640	70.9	2.638	134.7	2.663	2.696
O3LYP	2.654	75.1	2.663	140.0	2.685	2.717
OLYP			2.743	151.7	2.763	2.786
B3LYP			2.694	141.8	2.720	2.752
BLYP			2.697	144.9	2.722	2.754
B98			2.691	142.9	2.717	2.749
B971			2.696	142.5	2.723	2.754
B972			2.694	145.2	2.722	2.753
G96V5LYP			2.682	144.3	2.707	2.737
MPWV5LYP			2.693	144.4	2.718	2.752
HCTH147			2.704	155.0	2.730	2.758
HCTH407			2.742	163.6	2.764	2.784
SCF[a]	2.687	69.1			2.720	2.764
CCSD(T)[b]	2.774	68.5			2.798	2.845
CCSD(T)[c]	2.651	68.3			2.661	2.708

[a]Reference 12.
[b]Reference 13.
[c]Reference 14.

II. THEORETICAL DETAILS

All computations were performed with the GAUSSIAN03 suite of programs.[19] A total of 23 DFT methods were used for geometry optimization and vibrational frequency analysis. In order to reduce the effects of errors caused by numerical integration, the ultrafine GAUSSIAN03 grid (99 590) was used throughout the study.

Two effective core potential (ECP) basis sets were implemented in this study. The smaller one is designated LANL2DZ (Los Alamos ECP plus DZ),[20] which for silver describes the 28 core electrons with a pseudopotential and the 19 valence $4s^24p^64d^{10}5s^1$ electrons with a $[5s,6p,4d/3s,3p,2d]$ basis set. The larger basis set is labeled SDD (Stuttgart-Dresden ECP plus DZ),[21] which also describes the 28 core electrons with a pseudopotential and the 19 valence $4s^24p^64d^{10}5s^1$ electrons with a much larger $[8s,7p,6d/6s,5p,3d]$ basis set. Both basis sets are commonly used for the theoretical study of transition metal complexes,[14,22–24] and the accuracy of them has been examined, for example, by Bagatur'yants *et al.*[25]

For the density functional methods, we would like to briefly address their differences in terms of the treatment of the exact uniform electron gas limit in the correlation functional. Becke[26] has suggested that the exact uniform electron gas limit is a minimal requirement that should be attained for correlation functionals. The reason is that the exact uniform electron gas is undeniably a legitimate and well-studied many-body problem; thus, no functional failing to attain this well-understood limit is entirely satisfactory. However, in achieving acceptable reliability for small molecular systems it has been argued that the uniform electron gas limit is not critical. Hence, this requirement is often removed, for example, in the correlation functionals of Colle and Salvetti (CS),[27] LYP,[8] B88,[10] and B97.[28] On the other hand, the Perdew-series correlation functionals, such as P86,[29] PW91,[30] PBE,[31] and TPSS[32] are based on local spin-density approximation (LSDA),[33] which does satisfy the uniform electron gas limit. To date, it is still unclear that whether the uniform electron gas limit is important for small metal clusters.

TABLE II. Bond lengths (in Å) and bond angles (in degrees) of Ag_3, Ag_3^-, and Ag_3^+ predicted by different DFT methods with the SDD basis set. Note that some functionals predict two minima for the $^2B_2$ ground state of Ag_3.

| | $Ag_3(C_{2v})$ | | | | $Ag_3^-(D_{3h})$ | $Ag_3^+(D_{\infty h})$ |
| | | | $^2B_2$ | | | |
	R	Angle	R	Angle	R	R
VSXC	2.658	70.6			2.671	2.703
PBEPBE	2.642	70.2	2.638	136.7	2.660	2.694
PBE1PBE	2.646	70.4			2.668	2.703
TPSSTPSS	2.627	68.5	2.622	134.4	2.642	2.677
PW91PW91	2.636	70.0	2.631	136.9	2.652	2.688
MPWPW91	2.640	70.5	2.636	137.4	2.658	2.693
MPW1PW91	2.645	70.6	2.643	120.3	2.666	2.702
MPWB95	2.638	69.1	2.634	142.4	2.655	2.686
OB95	2.652	70.9	2.666	156.5	2.683	2.704
B1B95	2.645	69.3	2.644	133.2	2.666	2.697
BP86	2.635	70.4	2.630	137.9	2.652	2.687
G96VP86	2.621	69.8	2.617	136.9	2.637	2.672
O3LYP	2.629	71.9	2.633	143.2	2.653	2.685
OLYP			2.707	166.4	2.726	2.750
B3LYP			2.670	144.8	2.692	2.728
BLYP			2.674	147.6	2.697	2.731
B98			2.668	147.0	2.690	2.723
B971	2.668	78.4	2.673	146.7	2.695	2.727
B972			2.667	150.3	2.690	2.724
G96V5LYP			2.660	145.9	2.682	2.716
MPWV5LYP			2.670	147.4	2.693	2.728
HCTH147			2.676	164.2	2.697	2.728
HCTH407			2.706[a]	180.0[a]	2.725	2.751
SCF[b]	2.687	69.1			2.720	2.764
CCSD(T)[c]	2.774	68.5			2.798	2.845
CCSD(T)[d]	2.651	68.3			2.661	2.708

[a]HCTH407/SDD predicts the linear structure ($^2\Sigma_u^+$ state) as the global minimum for the neutral Ag_3 molecule.
[b]Reference 12.
[c]Reference 13.
[d]Reference 14.

III. RESULTS AND DISCUSSION

A. Structures of Ag_3^+ and Ag_3^-

All 23 DFT methods with both basis sets yielded a linear global minimum for the anion Ag_3^-, and an equilateral triangle structure for the cation Ag_3^+ (Tables I and II). For the open-shell neutral Ag_3, the Renner-Teller deformation leads to isosceles triangular global minima (C_{2v} symmetry, $^2B_2$ ground electronic state) with all DFT methods. This is in qualitative agreement with earlier experimental and theoretical studies.[12–14,34–36]

B. Neutral silver trimer structures

Based on the predicted Ag–Ag–Ag bond angle for the neutral silver trimer at the $^2B_2$ electronic state, the present DFT results may be divided into two distinct groups (Tables I and II). The methods in the first group predict a genuine minimum with an acute Ag–Ag–Ag bond angle ($\sim 70°$), in agreement with the previous high-level theoretical studies.[12–14] This group includes 13 DFT methods, i.e., those containing Perdew-Wang's correlation functional [PW91PW91 (Ref. 30) and MPW1PW91 (Ref. 37)], the

Perdew-Burke-Ernzehof correlation functional [PBEPBE and PBE1PBE (Ref. 31)], the Tao-Perdew-Staroverov-Scuseria correlation functional [TPSS (Ref. 32)], the Perdew 1986 correlation functional [BP86 (Refs. 10 and 29) and G96VP86 (Refs. 29, 33, and 38)], and the Becke 1995 correlation functional[26] [MPWB95 (Refs. 26 and 37) and B1B95 (Ref. 26)]. Van Voorhis and Scuseria's standalone functional VSXC (Ref. 39) is also classified in this group. The second group does not find the acute-angle structure, and geometry optimization leads only to the obtuse-angle structure ($\sim 140°$). This group includes ten DFT methods with the LYP correlation functional [BLYP, B3LYP, G96V5LYP,[8,33,38] MPWV5LYP,[8,33,37] and OLYP (Refs. 7 and 8)] as well as variations of Becke's 1997 functional[28] [B971,[40] B972,[41] and B98 (Ref. 42)], HCTH147,[43] and HCTH407.[44] The O3LYP method for Ag_3 is an exception, which does not behave like the other functionals containing the LYP correlation functional (group two), but rather like those in group one (Tables I and II).

With the 13 first-group DFT methods, the size of the ECP basis sets is not critical. The LANL2DZ and SDD basis sets yield theoretical geometries for neutral Ag_3 in good agreement with each other and with higher level theoretical

TABLE III. Relative energies (in kcal/mol) for Ag_3 predicted with the LANL2DZ and SDD basis sets.

	LANL2DZ		SDD	
	$^2B_2$		$^2B_2$	
	Acute	Obtuse	Acute	Obtuse
VSXC	0.0	0.7	0.0	
PBEPBE	0.0	0.1	0.0	0.0
PBE1PBE	0.0		0.0	
TPSSTPSS	0.0	0.9	0.0	0.9
PW91PW91	0.0	0.1	0.0	<0.1
MPWPW91	0.0	−0.1	0.0	−0.2
MPW1PW91	0.0		0.0	0.8
MPWB95	0.0	0.6	0.0	0.5
OB95	0.0	−0.2	0.0	−0.4
B1B95	0.0	1.2	0.0	1.4
BP86	0.0	−0.3	0.0	−0.4
G96VP86	0.0	<0.1	0.0	−0.2
O3LYP	0.0	−0.4	0.0	−0.5
OLYP		0.0		0.0
B3LYP		0.0		0.0
BLYP		0.0		0.0
B98		0.0		0.0
B971		0.0	0.7	0.0
B972		0.0		0.0
G96V5LYP		0.0		0.0
MPWV5LYP		0.0		0.0
HCTH147		0.0		0.0
HCTH407		0.0		0.0[a]

[a]The HCTH407/SDD method predicts the linear structure ($^2\Sigma_u^+$) to be the global minimum, instead of the $^2B_2$ state.

results for the acute structure. In going from the LANL2DZ to the SDD basis set, the obtuse angles slightly increase while the acute angles slightly decrease (Tables I and II). Most first-group methods predict two minima, one around 70° and another one around 140°. These two structures are nearly degenerate in energy ($\Delta E < 1.5$ kcal/mol, Table III). Most methods prefer the acute-angle structure, but a few functionals (O3LYP, BP86, OB95,[7,26] and MPWPW91) predict the obtuse-angle structure to have a lower energy by a marginal amount (<0.5 kcal/mol, Table III), and the two $^2B_2$ minima are exactly degenerate at PBE/SDD level. Figure 1(a) is the energy curve for the PW91PW91/LANL2DZ method and shows two energy minima at bond angles of 71° and 134°, separated by a small energy barrier of ~0.2 kcal/mol. Some DFT methods, namely, PBE1PBE with both basis sets, MPW1PW91/LANL2DZ, and VSXC/SDD, predict only one minimum at the acute bond angle of ~70°. Figure 1(b) shows the energy curve predicted by the PBE1PBE/LANL2DZ method, which shows only a single minimum at ~72° along with a shoulder at ~130°.

The prediction of a single Ag_3 minimum near $\theta = 70°$ best agrees with our own coupled-cluster results using the MOLPRO program.[45] The UCCSD/SDD method predicts a single equilibrium geometry at $r = 2.690$ Å and $\theta = 68.2°$, while the UCCSD(T)/SDD method predicts $r = 2.684$ Å and $\theta = 67.5°$. We have also carried out all-electron (no effective potential) computations using the Hartree-Fock and UCCSD
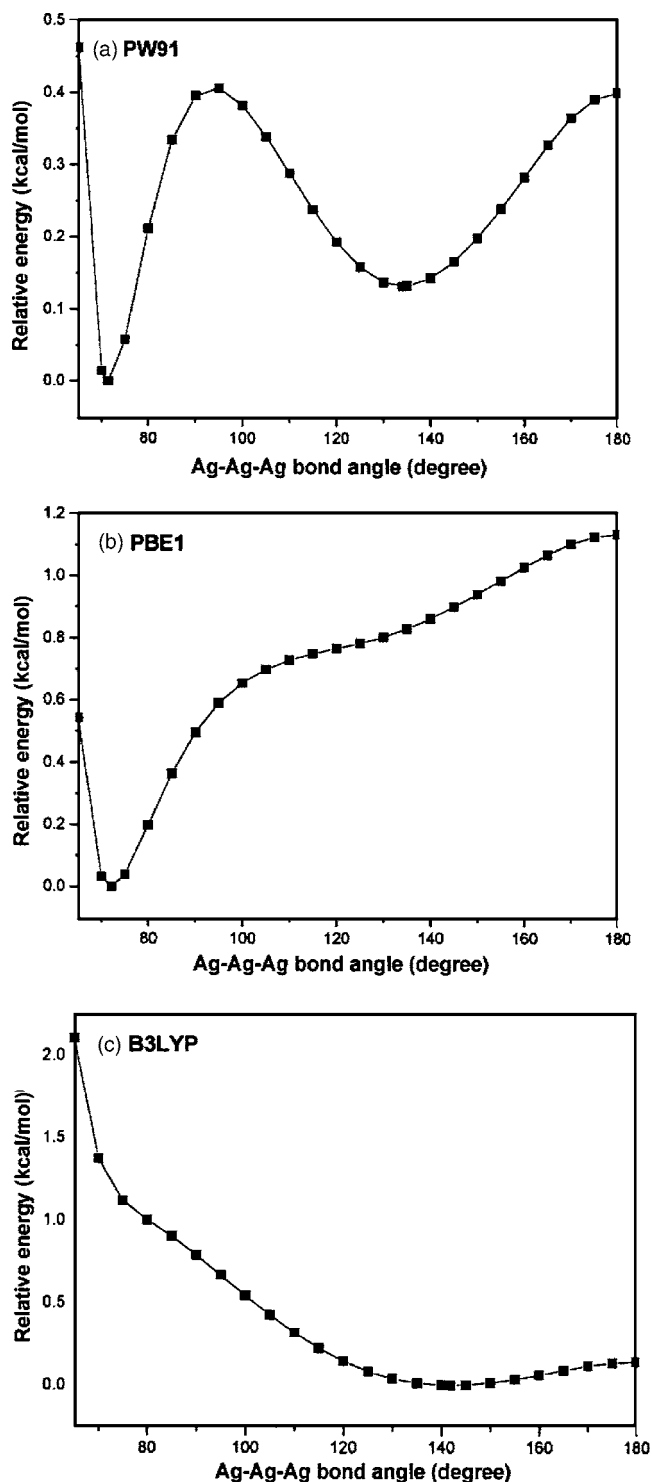

FIG. 1. The potential energy curve for the $^2B_2$ state of the neutral silver trimer as a function of the central Ag–Ag–Ag angle with (a) PW91PW91/LANL2DZ, (b) PBE1PBE/LANL2DZ, and (c) B3LYP/LANL2DZ.

methods with Huzinaga's Ag basis, the loosely contracted (4 332 121/4321/421) set plus two sets of diffuse p functions $\alpha_p = (0.118, 0.039)$.[46] With this all-electron basis set, the HF method predicts only one minimum at $r = 2.851$ Å and $\theta = 74.2°$, while the UCCSD method predicts $r = 2.743$ Å and $\theta = 67.6°$. The previous self-consistent field[12] (SCF) and CCSD(T) studies[13,14] also predict the acute apex angle to be ~70°.
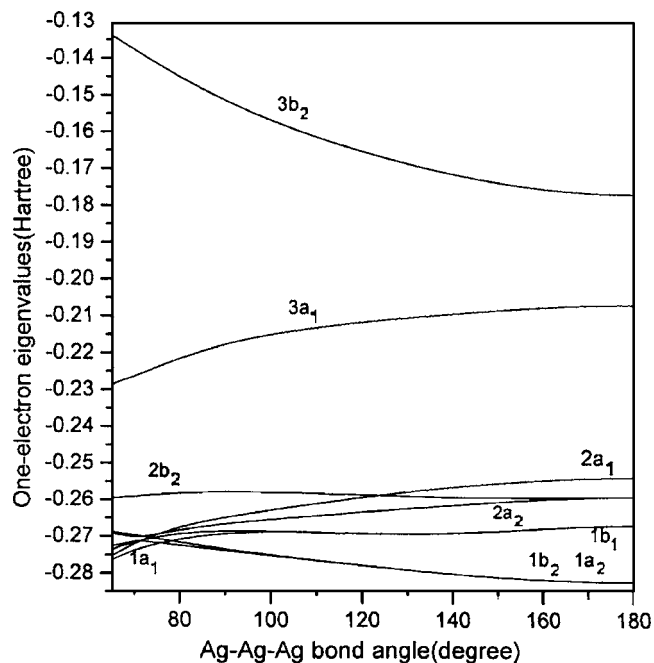
FIG. 2. The Walsh diagram for the $^2B_2$ state of the neutral silver trimer predicted by PW91PW91/LANL2DZ.

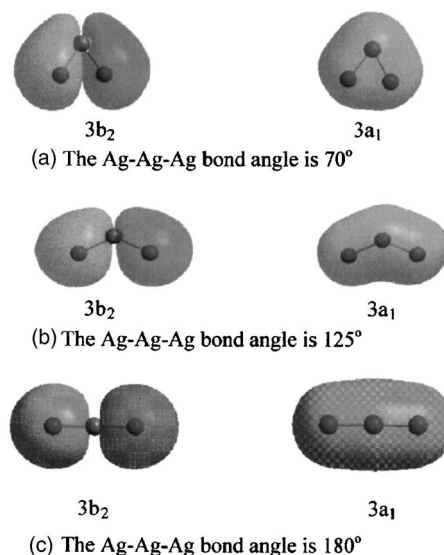FIG. 3. The MOs of Ag$_3$. (a) The Ag–Ag–Ag bond angle is 70°; (b) the Ag–Ag–Ag bond angle is 120°; (c) the Ag–Ag–Ag bond angle is 180°.

With the second group of DFT methods, the optimized geometry for neutral Ag$_3$ has only one minimum, but that with an obtuse bond angle around ∼140°. Figure 1(c) shows the energy curve predicted by the B3LYP/LANL2DZ method. The latter curve shows that there is no acute minimum but a shoulder near ∼70°. The exception among methods that do not incorporate the uniform electron gas limit, besides O3LYP (both basis sets), is the B971/SDD method, which also gives two minima, with the structure at 78.4°

TABLE IV. Relative energies in (kcal/mol) of different structures for Ag$_4^-$.

	LANL2DZ				SDD			
	$D_{2h}(^2B_{2u})$	$D_{\infty h}(^2\Sigma_g^+)$	$C_{2v}(^2B_2)$	$T_d(^4A_1)$	$D_{2h}(^2B_{2u})$	$D_{\infty h}(^2\Sigma_g^+)$	$C_{2v}(^2B_2)$	$T_d(^4A_1)$
VSXC	0.0	6.9	6.4	24.4	0.0	5.4	5.7	22.6
PBEPBE	0.0	2.1	2.3	17.9	0.0	1.4	2.0	18.3
PBE1PBE	0.0	1.9	1.8	14.5	0.0	1.8	1.8	14.6
TPSSTPSS	0.0	3.9	3.1	15.9	0.0	3.4	2.9	15.9
PW91PW91	0.0	2.2	2.4	18.0	0.0	1.6	2.1	18.3
MPWPW91	0.0	1.3	1.8	17.5	0.0	0.7	1.6	17.9
MPW1PW91	0.0	1.2	1.4	14.1	0.0	1.2	1.4	14.2
MPWB95	0.0	3.7	3.3	18.9	0.0	2.9	3.0	19.0
OB95	0.0	0.3	1.5	16.4	0.0	−0.1	1.3	16.2
B1B95	0.0	3.2	2.6	15.2	0.0	3.1	2.6	15.1
BP86	0.0	1.1	1.8	18.4	0.0	0.5	1.6	18.8
G96VP86	0.0	0.8	1.5	16.0	0.0	0.4	1.3	16.6
O3LYP	0.3	0.0	1.3	18.7	0.5	0.0	1.5	18.9
OLYP	5.7	0.0	3.9	25.5	6.6	0.0	4.5	26.5
B3LYP	2.4	0.0	2.2	21.5	2.9	0.0	2.5	22.2
BLYP	3.1	0.0	2.8	24.9	4.1	0.0	3.4	26.3
B98	1.6	0.0	2.5	24.7	1.9	0.0	2.7	24.4
B971	1.0	0.0	2.3	24.8	1.5	0.0	2.5	24.5
B972	2.3	0.0	3.1	26.8	2.5	0.0	3.1	26.1
G96V5LYP	3.5	0.0	2.8	23.8	4.2	0.0	3.3	25.2
MPWV5LYP	2.5	0.0	2.5	24.8	3.4	0.0	3.2	26.1
HCTH147	4.8	0.0	4.7	32.2	5.4	0.0	4.9	31.4
HCTH407	5.9	0.0	4.7	29.3	6.8	0.0	5.2	29.2

TABLE V. Vertical ionization potentials (VIPs), adiabatic ionization potentials (AIPs), and vertical detachment energies (VDEs) (in eV) of the silver trimer and tetramer with the LANL2DZ basis set. Note that VIP values for the trimer and the VDE values for the tetramer anion are divided into two groups.

	Trimer			Tetramer		
	VIP	AIP	VDE	VIP	AIP	VDE
VSXC	5.72	5.56	2.20	6.47	6.46	1.60
PBEPBE	5.95	5.79	2.23	6.53	6.52	1.71
PBEIPBE	5.71	5.53	2.03	6.23	6.22	1.53
TPSSTPSS	5.69	5.57	2.06	6.34	6.33	1.52
PW91PW91	6.02	5.85	2.29	6.60	6.59	1.77
MPWPW91	6.83	5.82	2.24	6.55	6.53	1.73
MPW1PW91	5.74	5.56	2.04	6.25	6.23	1.55
MPWB95	5.87	5.73	2.22	6.55	6.54	1.63
OB95	6.39	5.33	1.81	6.06	6.04	1.26
B1B95	5.58	5.44	1.99	6.21	6.19	1.42
BP86	6.99	5.96	2.39	6.69	6.68	1.87
G96VP86	6.03	5.88	2.29	6.59	6.58	1.79
O3LYP	6.66	5.60	2.06	6.32	6.31	1.97
OLYP	6.47	5.57	1.87	6.08	6.06	1.78
B3LYP	6.83	5.81	2.23	6.43	6.42	2.15
BLYP	6.84	5.90	2.22	6.50	6.49	2.09
B98	6.62	5.54	2.14	6.31	6.30	1.99
B971	6.56	5.49	2.11	6.28	6.27	1.94
B972	6.48	5.38	2.04	6.19	6.18	1.86
G96V5LYP	6.79	5.82	2.14	6.42	6.41	2.03
MPWV5LYP	6.88	5.94	2.27	6.57	6.55	2.12
HCTH147	6.80	5.81	2.29	6.52	6.50	2.09
HCTH407	6.82	5.88	2.24	6.34	6.42	2.12
Expt.	6.20,[a] 5.66[b]		2.4[c]	6.65[a]		1.63[c]

[a]Reference 48.
[b]Reference 49.
[c]Reference 50.

TABLE VI. Vertical ionization potentials (VIPs), adiabatic ionization potentials (AIPs), and vertical detachment energies (VDEs) (in eV) of the silver trimer and tetramer with the SDD basis set. Note that the VIP values for the trimer and the VDE values for the tetramer anion are divided into two groups.

	Trimer			Tetramer		
	VIP	AIP	VDE	VIP	AIP	VDE
VSXC	5.95	5.79	2.37	6.63	6.62	1.76
PBEPBE	6.10	5.97	2.42	6.71	6.70	1.82
PBE1PBE	5.81	5.67	2.19	6.39	6.37	1.62
TPSSTPSS	5.87	5.76	2.25	6.53	6.52	1.64
PW91PW91	6.17	6.03	2.47	6.78	6.77	1.87
MPWPW91	7.03	6.00	2.42	6.72	6.71	1.83
MPW1PW91	5.84	5.69	2.19	6.40	6.38	1.63
MPWB95	6.04	5.91	2.40	6.72	6.71	1.74
OB95	6.64	5.52	1.98	6.25	6.24	1.87
B1B95	5.71	5.58	2.15	6.36	6.34	1.51
BP86	7.18	6.14	2.58	6.87	6.86	1.98
G96VP86	7.11	6.06	2.46	6.76	6.75	1.89
O3LYP	6.86	5.76	2.22	6.48	6.47	2.12
OLYP	6.73	5.76	2.04	6.27	6.25	1.95
B3LYP	7.01	5.95	2.39	6.59	6.57	2.31
BLYP	7.04	6.08	2.41	6.68	6.67	2.26
B98	6.82	5.69	2.28	6.46	6.44	2.15
B971	6.76	5.64	2.26	6.43	6.41	2.11
B972	6.69	5.54	2.18	6.34	6.32	2.02
G96V5LYP	6.97	6.00	2.32	6.59	6.58	2.20
MPWV5LYP	7.08	6.12	2.46	6.74	6.73	2.30
HCTHI47	7.05	6.02	2.45	6.69	6.67	2.27
HCTH407	7.08[a]	6.10[a]	2.41	6.63	6.61	2.31
Expt.	6.20,[b] 5.66[c]		2.4[d]	6.65[b]		1.63[d]

[a]VIP and AIP at the HCTH407/SDD levels are based on the linear $Ag_3(^2\Sigma_u^+)$ structure.
[b]Reference 48.
[c]Reference 49.
[d]Reference 50.

higher in energy than that for the obtuse bond angle structure (Table III). Another special case is the HCTH407 method. The HCTH407/LANL2DZ method gives the widest apex angle, ~164°, while the HCTH407/SDD method predicts a linear structure (in its $^2\Sigma^+$ state). The Ag_3 structures from the second group of DFT methods are not in agreement with the high-level *ab initio* results. This abnormal phenomenon was also reported by Matulis *et al.*[16] in 2003 by using the B3LYP, BLYP, and G96LYP (Refs. 8 and 38) methods.

Walsh diagrams[47] are powerful tools for the rationalization of molecular geometries based on the properties of molecular orbitals. Figure 2 shows the Walsh diagram given by the PW91PW91/LANL2DZ method. In the diagram, we considered the nine highest occupied molecular orbitals ($1a_2$, $1b_2$, $1a_1$, $1b_1$, $2a_2$, $2a_1$, $2b_2$, $3a_1$, and $3b_2$). It seems that the Ag–Ag–Ag bond angle mainly depends on the highest two orbitals ($3a_1$ and $3b_2$), which qualitatively originate from the three 5s orbitals of the Ag atoms. Both $3a_1$ and $3b_2$ orbitals are bonding orbitals (see Fig. 3). The $3a_1$ orbital drops in energy as the molecule is bent from 180° to 60°, while the $3b_2$ orbital increases in energy. For the Ag_3^+ cation, the $3a_1$ orbital is doubly occupied while the $3b_2$ orbital is empty, so the $3a_1$ orbital directs the Ag_3^+ cation to its 60° bond angle (equilateral triangle). For the Ag_3^- anion, both orbitals $3a_1$

and $3b_2$ are doubly occupied and the $3b_2$ orbital drops in energy (from 60° to 180°) more rapidly, and thus the structure of Ag_3^- is linear. For neutral Ag_3, there is only one electron, instead of two, in the $3b_2$ orbital, and the influence of this orbital will be only half as much as for the anion. Because of the compensating effect of the $3b_2$ and $3a_1$ orbitals as a function of the Ag_3 angle, the Walsh diagrams do not allow us to rationalize the differences between the PW91PW91, PBE1PBE, and B3LYP functionals.

Nevertheless, by examining the structure of the 23 functionals investigated, together with their predicted Ag_3 geometries, we may generalize as follows. First, the correlation functionals attaining the limit of the *exact uniform electron gas* (i.e., slowly varying density) are P86, B95, PW91, PBE, and TPSS. The latter methods generally predict better geometries compared to the others, such as the LYP correlation functional, which is formulated from the Hartree-Fock density,[8] and the B97 functional constructed with fully optimized XC parameters. This is quite surprising, implying that even the smallest Ag cluster (Ag_3) already behaves metallic-like to some extent due to the extended 5s orbital of Ag. Second, the incorporation of *the exact exchange* will also help to stabilize the acute-angle geometry. For example, the

B3LYP and O3LYP functionals share the same correlation part and differ only because of the replacement of the B88 exchange by the OPTX exchange. The latter method, OPTX,[7] was constructed to produce a more accurate HF exchange energy for atoms than the B88 functional. As also noticed, the PBE1PBE mainly differs from the PW91PW91 and PBEPBE in the exchange functional. The PBE1PBE method incorporates the exact exchange and the Slater exchange.[31] This addition results in a single true minimum from PBE1PBE, distinct from the two minima predicted by both PW91PW91 and PBEPBE. In conclusion, from our analysis we believe that the correlation functional derived from the uniform electron gas is vital to correctly describing the structure of the Ag clusters, and the addition of exact exchange may further improve the results.

C. Structure of Ag$_4$

All the functionals with both LANL2DZ and SDD basis sets predict the global minimum for the neutral and cationic silver tetramer to be a rhombic structure (D_{2h}).

For the anionic tetramer Ag$_4^-$, the DFT methods predict four local minima (Table IV), which are three doublet structures (D_{2h}, $D_{\infty h}$, and C_{2v}) and one quartet structure (T_d). Similar to the situation for the neutral Ag$_3$ cluster, the DFT methods may be divided into two groups. The first group of methods (the same as those for the neutral Ag$_3$ except O3LYP) predicts the rhombic structure (D_{2h}) of Ag$_4^-$ to be the global minimum, in agreement with earlier theoretical [configuration interaction (CI) (Ref. 15) and CCSD (Ref. 13)] studies. However, the second group (the same group of functionals considered for neutral Ag$_3$ plus O3LYP) predicts the linear structure ($D_{\infty h}$) to be the global minimum (Table IV). The OB95/SDD method is an exception, predicting the linear structure to lie lower than the rhombic structure by only 0.1 kcal/mol. Note that for the anionic tetramer, the O3LYP method rejoins the less well performing second group, which includes the other LYP-containing functionals.

D. Energetic properties of Ag$_3$ and Ag$_4$

Experimental ionization potential (IP) energies for trimer [6.20 eV (Ref. 48) and 5.66 eV (Ref. 49)] and tetramer [6.65 eV (Ref. 48)] were reported in 1990s.

As discussed above (Tables I and II), the different functionals predict two distinct structures for the neutral trimer: one with an acute apex angle ($\sim 70°$) and another with an obtuse angle ($\sim 140°$). Table III shows that the energies for these two structures are nearly degenerate. Hence all the DFT methods predict similar values for the AIP (Tables V and VI). However, the VIP strongly depends on the geometry of the neutral species. The functionals (mainly the first group), which give the acute apex angle for the neutral trimer, predict VIP values (5.6–6.0 eV with the LANL2DZ basis set or 5.7–6.2 eV with the SDD basis set; see Tables V and VI) somewhat below the experimental VIP, while the functionals (mainly the second group), which give the obtuse apex angle for neutral trimer, predict higher VIP values (6.4–7.0 eV with the LANL2DZ basis set or 6.6–7.2 eV with the SDD basis set). This is understandable, since the

TABLE VII. Theoretical ionization potentials (IPs) and electron affinities (EAs, in eV) for the Ag atom.

	IP		EA	
	LANL2DZ	SDD	LANL2DZ	SDD
VSXC	7.44	7.74	1.13	1.49
PBEPBE	7.78	8.06	1.06	1.39
PBE1PBE	7.52	7.73	0.85	1.15
TPSSTPSS	7.54	7.83	0.89	1.22
PW91PW91	7.85	8.13	1.11	1.43
MPWPW91	7.81	8.09	1.07	1.38
MPW1PW91	7.54	7.76	0.85	1.14
MPWB95	7.72	8.01	1.07	1.40
OB95	7.28	7.56	0.67	1.04
B1B95	7.43	7.64	0.83	1.13
BP86	7.92	8.22	1.25	1.55
G96VP86	7.86	8.16	1.13	1.40
O3LYP	7.59	7.83	0.91	1.22
OLYP	7.42	7.70	0.75	1.12
B3LYP	7.75	7.97	1.09	1.38
BLYP	7.81	8.09	1.10	1.43
B98	7.42	7.65	1.05	1.34
B971	7.37	7.60	1.02	1.32
B972	7.22	7.46	0.98	1.27
G96V5LYP	7.73	8.02	1.01	1.31
MPWV5LYP	7.86	8.13	1.15	1.48
HCTH147	7.55	7.86	1.30	1.59
HCTH407	7.57	7.91	1.27	1.59
Expt.[a]	7.576		1.302	

[a]Reference 51.

acute apex angle for the neutral trimer ($\sim 70°$) is close to $60°$, which is the apex angle for the energy minimum of the cationic trimer. The obtuse apex angle ($\sim 140°$) is far from the $60°$ apex angle for the cationic trimer equilibrium geometry, and a higher energy is expected for Ag$_3^+$ at the structure with the obtuse apex angle. Consequently, the first group of functionals predicts VIPs for Ag$_3$ lower than that for Ag$_4$, and this is in agreement with experiment.[48] However, the second group of functionals predicts the opposite result.

The experimental VDE for the anionic tetramer Ag$_4^-$ has been reported to be 1.63 eV.[50] The DFT methods in the first group, which predict the global minimum of Ag$_4^-$ to be a D_{2h} structure (Table IV), predict reasonable VDE values (<2.0 eV and most of them in the range of 1.5–1.8 eV; Tables V and VI). However, the DFT methods in the second group, which find the global minimum of Ag$_4^-$ to be linear (Table IV), predict much higher VDE values (most of them >2.0 eV) for the tetramer anion (Tables V and VI). The reason for the latter problem is analogous to that for the trimer VIP; the VDE value is smaller when the anion structure is similar to that for the neutral, and the VDE should be larger when the anion structure is far different from the neutral. In summary, the DFT methods are divided into two groups for predicting the energetic properties (VIP and VDE), just as they predict different geometries.

E. Properties of the silver atom and the silver dimer

To complete the present study, we have also investigated the silver atom and silver dimer with the same 23 DFT meth-

TABLE VIII. Bond distances (in Å), harmonic vibrational frequencies (in cm^{-1}), binding energies (E_b, in eV), vertical ionization potentials (VIPs, in eV), adiabatical ionization potentials (AIPs, in eV), and vertical detachment energies (VDEs, in eV) for the silver dimer and its ions by using different DFT methods with the LANL2DZ basis set.

	Ag$_2$					Ag$_2^+$		Ag$_2^-$		
	R	Frequency	E_b	VIP	AIP	E_b	Frequency	E_b	Frequency	VDE
VSXC	2.579	189	2.15	7.89	7.82	1.76	135	1.74	135	0.78
PBEPBE	2.590	183	1.76	7.89	7.82	1.72	129	1.66	134	1.02
PBE1PBE	2.594	182	1.52	7.53	7.45	1.59	123	1.52	131	0.91
TPSSTPSS	2.575	187	1.73	7.67	7.59	1.67	129	1.65	139	0.86
PW91PW91	2.584	185	1.78	7.96	7.89	1.73	130	1.69	136	1.07
MPWPW91	2.586	184	1.70	7.90	7.83	1.68	128	1.62	135	1.04
MPW1PW91	2.592	183	1.48	7.54	7.46	1.56	122	1.49	131	0.93
MPWB95	2.583	185	1.86	7.93	7.86	1.72	132	1.67	134	0.93
OB95	2.609	169	1.50	7.38	7.30	1.48	105	1.40	117	0.63
B1B95	2.589	184	1.57	7.52	7.44	1.56	129	1.48	131	0.79
BP86	2.579	186	1.75	8.05	7.98	1.70	131	1.63	136	1.18
G96VP86	2.563	190	1.59	7.92	7.84	1.60	132	1.53	139	1.13
O3LYP	2.585	181	1.64	7.68	7.60	1.63	122	1.52	128	0.85
OLYP	2.647	159	1.42	7.45	7.37	1.48	98	1.34	104	0.73
B3LYP	2.612	177	1.55	7.79	7.72	1.58	121	1.45	123	1.05
BLYP	2.618	175	1.69	7.91	7.84	1.65	123	1.53	124	1.00
B98	2.614	176	1.79	7.67	7.60	1.61	116	1.51	110	0.84
B971	2.619	176	1.83	7.64	7.58	1.62	116	1.53	110	0.79
B972	2.609	176	1.81	7.55	7.48	1.55	122	1.46	119	0.71
G96V5LYP	2.601	179	1.55	7.80	7.73	1.55	122	1.43	126	0.95
MPWV5LYP	2.616	176	1.77	7.98	7.92	1.71	125	1.59	125	1.03
HCTH147	2.617	169	1.94	7.93	7.86	1.62	119	1.53	111	0.96
HCTH407	2.644	156	1.84	7.85	7.79	1.62	108	1.54	93	1.06
Expt.	2.531[a]	192[a]	1.66[b]	7.60[c]	7.656[b]	1.74[d]	136[e]	1.37[f]	145.0[f]	1.10[g]

[a]Reference 53.
[b]Reference 52.
[c]Reference 48.
[d]Reference 54.
[e]Reference 56.
[f]Reference 55.
[g]Reference 50.

ods. Table VII shows that the IPs of the silver atom predicted by the 23 DFT methods is in the range of 7.2–7.9 eV with the LANL2DZ basis set, or 7.5–8.2 eV with the SDD basis set, in good agreement with the experimental result [7.6 eV (Ref. 51)]. The electron affinity (EA) is predicted to be 0.7–1.3 eV (LANL2DZ) or 1.0–1.6 eV (SDD). Compared to experimental EA of 1.30 eV,[51] the DFT results with the SDD basis set are in better agreement than those with the smaller LANL2DZ basis set. No significant gap allows us to separate these DFT methods into two groups as was done for the trimer and tetramer. Note that the OB95/LANL2DZ method predicts an EA (0.67 eV) for the Ag atom that is unreasonably low, but the larger basis set OB95/SDD result is much better, 1.04 eV.

The 23 DFT methods were used to investigate the structural and energetic properties for the dimers Ag$_2$, Ag$_2^+$, and Ag$_2^-$ (Tables VIII and IX), in the thought that they might be divided into two groups analogous to those for the trimer. However, the gaps in the theoretical results between the two groups are not as significant as those for the trimer (Tables I and II). The first-group methods (with the P86, B95, PW91, PBE, and TPSS correlation functionals) predict vibrational frequencies in the range of 181–190 cm^{-1} (except OB95),

close to the experimental result (192 cm^{-1}).[52] Among these the BP86 and G96P86 methods predict the frequencies closest to experiment. The second-group DFT methods (with the LYP correlation functional and those related to the B97 functional) predict lower vibrational frequencies in the range of 159–179 cm^{-1}, among which the HCTH407 and OLYP methods with LANL2DZ predict it the lowest (156 and 159 cm^{-1}, respectively). Not surprisingly, the first-group DFT methods predict shorter Ag–Ag bond distances, which are closer to the experimental result [2.531 Å (Ref. 53)] than the second-group methods (Tables VIII and IX). For the binding energies with the neutral and ionic silver dimer, the VSXC method overestimates them, except for Ag$_2^+$ with the VSXC/LANL2DZ method.[52,54,55] In the earlier testing of Schultz *et al.* of the performance of DFT methods on eight transition metal dimers, hybrid methods were found to generally perform worse than pure GGA functionals.[6] BLYP and G96LYP, which contain the LYP correlation functional, are the best methods on calculating the atomization energies of the eight dimers. However, for the silver dimer atomization energies alone, Tables VIII and IX indicate that there is no distinct difference between hybrid and pure GGA functions. In going from the LANL2DZ to the SDD basis set, the VIP,

TABLE IX. Bond distances (in Å), harmonic vibrational frequency (in cm^{-1}), binding energies (E_b, in eV), vertical ionization potentials, (VIPs, in eV), adiabatic ionization potentials (AIPs, in eV), and vertical detachment energies (VDEs, in eV) for silver dimer and its ions by using different DFT methods with the SSD basis set.

	Ag$_2$					Ag$_2^+$		Ag$_2^-$		
	R	Frequency	E_b	VIP	AIP	E_b	Frequency	E_b	Frequency	VDE
VSXC	2.580	184	2.10	8.06	8.00	1.84	131	1.54	129	1.00
PBEPBE	2.576	185	1.75	8.07	8.01	1.79	130	1.48	135	1.17
PBE1PBE	2.576	185	1.52	7.67	7.60	1.64	125	1.35	133	1.03
TPSSTPSS	2.561	190	1.71	7.86	7.80	1.74	132	1.47	140	1.02
PW91PW91	2.570	187	1.77	8.14	8.09	1.81	132	1.51	137	1.22
MPWPW91	2.573	186	1.69	8.08	8.02	1.76	130	1.45	136	1.19
MPW1PW91	2.575	186	1.47	7.68	7.61	1.62	124	1.33	134	1.05
MPWB95	2.572	186	1.84	8.10	8.04	1.80	131	1.48	135	1.09
OB95	2.588	174	1.47	7.58	7.50	1.53	111	1.17	121	0.79
BIB95	2.574	186	1.56	7.66	7.58	1.61	126	1.31	133	0.93
BP86	2.568	187	1.73	8.23	8.17	1.78	132	1.46	136	1.33
G96VP86	2.555	190	1.58	8.11	8.04	1.69	133	1.39	140	1.26
O3LYP	2.565	184	1.61	7.83	7.76	1.68	124	1.33	131	0.99
OLYP	2.621	164	1.37	7.63	7.56	1.51	100	1.09	109	0.90
B3LYP	2.596	179	1.52	7.94	7.87	1.63	121	1.26	125	1.18
BLYP	2.605	176	1.66	8.08	8.02	1.72	123	1.33	124	1.16
B98	2.595	176	1.74	7.80	7.73	1.66	120	1.32	120	0.99
B971	2.600	175	1.79	7.77	7.71	1.68	120	1.35	119	0.94
B972	2.590	179	1.76	7.69	7.61	1.61	123	1.28	122	0.86
G96VSLYP	2.591	179	1.54	7.98	7.92	1.64	124	1.26	127	1.08
MPWV5LYP	2.602	177	1.73	8.15	8.09	1.77	125	1.38	125	1.19
HCTH147	2.599	172	1.85	8.09	8.03	1.68	120	1.32	114	1.13
HCTH407	2.618	164	1.68	8.02	7.95	1.64	109	1.26	104	1.25
Expt.	2.531[a]	192[a]	1.66[b]	7.60[c]	7.656[b]	1.74[d]	136[e]	1.37[f]	145.0[f]	1.1[g]

[a]Reference 53.
[b]Reference 52.
[c]Reference 48.
[d]Reference 54.
[e]Reference 56.
[f]Reference 55.
[g]Reference 50.

AIP, and VDE values increase, consistent with an earlier study.[16] All the functionals with the SDD basis set overestimate the VIP and AIP values, but they predict reasonable VDEs compared to experiment. The best performance for the IP is provided by OLYP/SDD (7.63 eV for VIP and 7.56 eV for AIP). The OB95 method underestimates the Ag$_2^-$ VDE for both the LANL2DZ and SDD basis sets.

IV. CONCLUSIONS: COMPARISON OF METHODS

We have compared a total of 23 DFT methods, including second- and the third-generation functionals, for their applications to the small silver clusters. Two basis sets (LANL2DZ and SDD) were employed. We find that these DFT methods may be generally divided into two groups according to their treatment of the correlation energy. The first group includes those with the P86, B95, PW91, PBE and TPSS correlation functionals, which satisfy the uniform electron gas limit in the correlation functional. The other group includes those with the LYP and B97 correlation functionals.

The first group of functionals (and O3LYP) with both the LANL2DZ and SDD basis sets predicts a minimum for the neutral silver trimer (Ag$_3$) in its $^2B_2$ electronic ground state with an acute apex angle ($\sim70°$). A separate minimum with an obtuse angle ($\sim140°$) is also predicted by most of the methods in this first group. However, the second group of functionals predicts only one (apparently spurious) minimum with an obtuse apex angle ($\sim140°$) for the neutral silver trimer. For the tetramer anion Ag$_4^-$, the first group of functionals predicts a rhombic (D_{2h} symmetry) global minimum, while the second group predicts a linear ($D_{\infty h}$ symmetry) global minimum.

The first group of DFT methods predicts more reasonable vertical ionization potentials (VIPs) for Ag$_3$, while the second group yields values that are too high (Tables V and VI). The VIPs for Ag$_3$ predicted by the second group are even higher than those for Ag$_4$, again inconsistent with experiment. Also, the first group predicts Ag$_4^-$ VDE values closer to the experimental result than those of the second group, which provide VDEs that are uniformly too high.

It should be noted that only PBE1PBE predicts a single equilibrium geometry (apex angle $\sim70°$) with both basis sets for Ag$_3$ in its $^2B_2$ electronic ground state. Therefore, PBE1PBE is the only functional that yields results com-

pletely consistent with the CI, CCSD, and CCSD(T) methods. PBE1PBE also yields more accurate energetic properties (IPs and VDEs) for the silver atom and dimer and performs reasonably well for the energetics of Ag_3 and Ag_4.

For the energetic properties of the larger clusters (Ag_3 and Ag_4), the PW91 GGA functionals (PW91PW91, MP-WPW91, and MPW1PW91) seem to give more accurate results (IPs and VDE) when compared to experiment. These functionals also predict more reliable vibrational frequencies for the silver dimer.

ACKNOWLEDGMENTS

[1] Y. Zhao, J. Pu, B. J. Lynch, and D. G. Truhlar, Phys. Chem. Chem. Phys. **6**, 673 (2004).

[2] Y. Zhao, B. J. Lynch, and D. G. Truhlar, J. Phys. Chem. A **108**, 2715 (2004).

[3] C. J. Barden, J. C. Rienstra-Kiracofe, and H. F. Schaefer, J. Chem. Phys. **113**, 690 (2000).

[4] S. Yanagisawa, T. Tsuneda, and K. Hirao, J. Chem. Phys. **112**, 545 (2000).

[5] J. Baker and P. Pulay, J. Comput. Chem. **24**, 1184 (2003).

[6] N. E. Schultz, Y. Zhao, and D. G. Truhlar, J. Phys. Chem. A **109**, 4388 (2005).

[7] N. C. Handy and A. J. Cohen, Mol. Phys. **99**, 403 (2001).

[8] C. Lee, W. Yang, and R. G. Parr, Phys. Rev. B **37**, 785 (1988); B. Miehlich, A. Savin, H. Stoll, and H. Preuss, Chem. Phys. Lett. **157**, 200 (1989).

[9] A. D. Becke, J. Chem. Phys. **98**, 5648 (1993).

[10] A. D. Becke, Phys. Rev. A **38**, 3098 (1988).

[11] X. Jin, L. Zhuang, and J. Lu, J. Electroanal. Chem. **519**, 137 (2002); P. A. Busch, S. P. Cheston, and D. S. Greywall, Cryogenics **24**, 445 (1984); A. P. Padilla, J. A. Rodríguez, and H. A. Saitúa, Desalination **114**, 203 (1997).

[12] V. Bonačić-Koutecký, L. Češpiva, P. Fantucci, and J. Koutecký, J. Chem. Phys. **98**, 7981 (1993).

[13] M. N. Huda and A. K. Ray, Eur. Phys. J. D **22**, 217 (2003).

[14] J. Yoon, K. S. Kim, and K. K. Baeck, J. Chem. Phys. **112**, 9335 (2000).

[15] V. Bonačić-Koutecký, L. Češpiva, P. Fantucci, and J. Koutecký, J. Chem. Phys. **100**, 490 (1994).

[16] V. E. Matulis, O. A. Ivashkevich, and V. S. Gurin, J. Mol. Struct. **664**, 291 (2003).

[17] R. Fournier, J. Chem. Phys. **115**, 2165 (2001).

[18] M. N. Huda, Phys. Rev. A **67**, 013201 (2003).

[19] M. J. Frisch, G. W. Trucks, H. B. Schlege *et al.*, GAUSSIAN 03, Revision B.03, Gaussian Inc., Pittsburgh, PA, 2003.

[20] P. J. Hay and W. R. Wadt, J. Chem. Phys. **82**, 270 (1985); W. R. Wadt and P. J. Hay, *ibid.* **82**, 284 (1985); P. J. Hay and W. R. Wadt, *ibid.* **82**, 299 (1985).

[21] D. Andrae, U. Haussermann, M. Dolg, H. Stoll, and H. Preuss, Theor. Chim. Acta **77**, 123 (1990).

[22] K. A. Bosnick, T. L. Haslett, S. Fedrigo, M. Moskovits, W.-T. Chan, and R. Fournier, J. Chem. Phys. **111**, 8867 (1999).

[23] C. W. Bauschlicher, S. R. Langhoff, and H. Partridge, J. Chem. Phys. **93**, 8133 (1990).

[24] V. Bonačić-Koutecký, J. Pittner, M. Boiron, and P. Fantucci, J. Chem. Phys. **110**, 3876 (1999).

[25] A. A. Bagatur'yants, A. A. Safonov, H. Stoll, and H.-J. Werner, J. Chem. Phys. **109**, 3096 (1998).

[26] A. D. Becke, J. Chem. Phys. **104**, 1040 (1996).

[27] R. Colle and O. Salvetti, J. Chem. Phys. **79**, 1404 (1983).

[28] A. D. Becke, J. Chem. Phys. **107**, 8554 (1997).

[29] J. P. Perdew, Phys. Rev. B **33**, 8822 (1986).

[30] J. P. Perdew, J. A. Chevary, S. H. Vosko, K. A. Jackson, M. R. Pederson, D. J. Singh, and C. Fiolhais, Phys. Rev. B **46**, 6671 (1992); J. P. Perdew, K. Burke, and Y. Wang, *ibid.* **54**, 16533 (1996).

[31] J. P. Perdew, K. Burke, and M. Ernzerhof, Phys. Rev. Lett. **77**, 3865 (1996); **78**, 1396 (1997).

[32] J. Tao, J. P. Perdew, V. N. Staroverov, and G. E. Scuseria, Phys. Rev. Lett. **91**, 146401 (2003); J. P. Perdew, J. Tao, V. N. Staroverov, and G. E. Scuseria, J. Chem. Phys. **120**, 6898 (2004).

[33] S. H. Vosko, L. Wilk, and M. Nusair, Can. J. Phys. **58**, 1200 (1980).

[34] H. M. Lee, M. Ge, B. R. Sahu, P. Tarakeshwar, and K. S. Kim, J. Phys. Chem. B **107**, 9994 (2003).

[35] A. M. Ellis, E. S. J. Robles, and T. A. Miller, Chem. Phys. Lett. **201**, 132 (1993).

[36] B. Miller, J. A. Howard, M. Histed, H. Morris, and C. A. Hampson, Faraday Discuss. **92**, 129 (1991).

[37] C. Adamo and V. Barone, J. Chem. Phys. **108**, 664 (1998).

[38] P. M. W. Gill, Mol. Phys. **89**, 433 (1996); C. Adamo and V. Barone, J. Comput. Chem. **19**, 419 (1998).

[39] T. Van Voorhis and G. E. Scuseria, J. Chem. Phys. **109**, 400 (1998).

[40] F. A. Hamprecht, A. J. Cohen, D. J. Tozer, and N. C. Handy, J. Chem. Phys. **109**, 6264 (1998).

[41] P. J. Wilson, T. J. Bradley, and D. J. Tozer, J. Chem. Phys. **115**, 9233 (2001).

[42] H. L. Schmider and A. D. Becke, J. Chem. Phys. **108**, 9624 (1998).

[43] A. D. Boese, N. L. Doltsinis, N. C. Handy, and M. Sprik, J. Chem. Phys. **112**, 1670 (2000).

[44] A. D. Boese and N. C. Handy, J. Chem. Phys. **114**, 5497 (2001).

[45] H.-J. Werner, P. J. Knowles, M. Schütz *et al.*, MOLPRO, a package of *ab initio* programs.

[46] S. Huzinaga, J. Andzelm, M. Klobukowski, E. Radzio-Andzelm, Y. Sakai, and H. Tatewaki, *Gaussian Basis Sets for Molecular Calculations* (Elsevier Science, New York, 1984), pp. 274 and 24.

[47] A. D. Walsh, J. Chem. Soc. (London) 2260, (1953); 2266, (1953).

[48] C. Jackschath, I. Rabin, and W. Schulze, Z. Phys. D **22**, 517 (1992).

[49] G. Alammeddin, J. Hunter, D. Cameron, and M. M. Kappes, Chem. Phys. Lett. **192**, 122 (1992).

[50] H. Handschuh, C.-Y. Cha, P. S. Bechthold, G. Ganteför, and W. Eberhardt, J. Chem. Phys. **102**, 6406 (1995).

[51] C. E. Moore, Natl. Bur. Stand. Circ. (U. S.) **3**, 467 (1958).

[52] K. P. Huber and G. Herzberg, *Molecular Spectra and Molecular Structure*, Constants of Diatomic Molecules Vol. IV (Van Nostrand, Toronto, 1979).

[53] B. Simard, P. A. Hackett, A. M. James, and P. R. R. Langridge-Smith, Chem. Phys. Lett. **186**, 415 (1991).

[54] S. Krückeberg, G. Dietrich, K. Lützenkirchen, L. Schweikard, G. Walther, and J. Ziegler, J. Chem. Phys. **110**, 7216 (1999).

[55] J. Ho, K. M. Ervin, and W. C. Lineberger, J. Chem. Phys. **93**, 6987 (1990).

[56] V. Beutel, G. L. Bhale, M. Kuhn, and W. Demtröder, Chem. Phys. Lett. **185**, 313 (1991).